BIOCELL

Tech Science Press

http://doi.org/10.32604/biocell.2026.079046

ARTICLE

Characterization of Alive and Impaired NET-Releasing Neutrophils in A Model of the Blood-Cerebrospinal Fluid Barrier after *Streptococcus suis* Infection

Laura Schaltz[1,2], Simon Lassnig[1,2], Karola Schlote[1,2], Christian Schwerk[3], Horst Schroten[3] and Nicole de Buhr[1,2,*]

[1]Institute of Biochemistry, University of Veterinary Medicine Hannover, Hannover, Germany
[2]Research Center for Emerging Infections and Zoonoses (RIZ), University of Veterinary Medicine Hannover, Hannover, Germany
[3]Department of Pediatrics, Pediatric Infectious Diseases, Medical Faculty Mannheim, Heidelberg University, Mannheim, Germany
*Corresponding Author: Nicole de Buhr. Email: nicole.de.buhr@tiho-hannover.de

Received: 13 January 2026; Accepted: 20 April 2026; Published: 27 July 2026

ABSTRACT: Objectives: *Streptococcus suis* (*S. suis*) is a worldwide occurring pathogen in pigs and humans that can cross the blood-cerebrospinal fluid barrier (BCSFB) to cause meningitis, while host neutrophils counter infection through mechanisms including the release of neutrophil extracellular traps (NETs). NET-formation involves the release of nuclear DNA with antimicrobial components, which can bind and kill bacteria. We aimed to characterize the host-pathogen interaction between *S. suis* and neutrophils within the CSF compartment, focusing on NET-formation. **Methods:** A 3D cell culture model of the porcine BCSFB was used by cultivating a porcine choroid plexus epithelial cell line (PCP-R) on filter inserts. Following *S. suis* infection, porcine neutrophils were added to the basolateral side. The study specifically focused on the quantification of alive and impaired NET-releasing neutrophils. Transmigrated neutrophils in the CSF compartment were stained for NETs and with Live-or-Dye NucFix™ and analyzed by confocal microscopy to quantify NET release and cell viability. **Results:** In uninfected samples, most transmigrated neutrophils remained NET-negative (96.9% SD ± 1.9%). In contrast, 46.9% (SD ± 12.9%) of neutrophils infiltrating the *S. suis*-infected CSF compartment exhibited NET formation. Only a minor fraction of NET-releasing cells remained alive (9.8% SD ± 8.7%), whereas the majority became impaired (Live-or-Dye positive). This process correlated with increased *S. suis* colony-forming units in the CSF compartment. However, Live-or-Dye positive neutrophils retained the ability to produce reactive oxygen species (ROS) in response to *S. suis*, although ROS production decreased after 4 h. **Conclusion:** Using a novel staining approach to distinguish NET formation and cell viability, we demonstrated that *S. suis* infection predominantly induces NET release in the CSF compartment in an *in vitro* model of the BCSFB after four hours. The majority of these NET-releasing neutrophils are impaired. This likely leads to a loss of the defense mechanisms of the neutrophils.

KEYWORDS: *Streptococcus suis*; neutrophil extracellular traps (NETs); impaired NET-activated; alive NET-activated; host-pathogen interaction; meningitis; blood-cerebrospinal fluid barrier

1 Introduction

Streptococcus suis (*S. suis*) is a gram-positive pathogen that causes sepsis, arthritis, and endocarditis in pigs [1]. It is a zoonotic pathogen, as humans can be infected [2], and an infection can cause meningitis in pigs and humans [1]. The pathogen is characterized by a wide variety of serotypes, with serotype 2 being the most prevalent among invasive isolates worldwide [1]. To cause meningitis, *S. suis* crosses the blood-cerebrospinal fluid barrier (BCSFB) and then spreads throughout the cerebrospinal fluid (CSF) [3].

The BCSFB consists of choroid plexus epithelial cells and tight junctions and is located in the ventricles [4]. It serves as a barrier primarily for water-soluble molecules and produces the majority of CSF. It also contains endothelial cells and immune cells for strong immune resilience [5].

As a first immune defense against *S. suis*, neutrophil granulocytes migrate from the blood into the CSF. They can be attracted by various cytokines and chemokines, for example, interleukin-8 (IL-8) [6]. Neutrophils are part of the innate immunity and have various mechanisms to counteract pathogens, such as phagocytosis and neutrophil extracellular trap (NET) formation [7,8]. NETosis leads to the release of DNA and histones, as well as various granule proteins and antimicrobial peptides. A *S. suis* infection also results in NET-formation, but various DNases (like *S. suis* nuclease A) can degrade the NETs at an early stage, thereby reducing the immune response [9,10]. For this reason, the phenotype of NETs formed can be important for immune resilience. Two phenotypes of NETs are known. There are vital and suicidal NETosis [11,12]. Vital NET-formation is a rapid and oxidative burst-independent mechanism. Vesicles containing part of the DNA are formed in the cell and leave it without destroying the plasma membrane. This keeps the neutrophils viable and still able to phagocytose [13]. In suicidal NETosis, an oxidative burst-dependent mechanism leads to a pre-lytic disruption of the nuclear membrane and mixing of nuclear content with cytoplasmic components. This is followed by the release of the content to the extracellular space and the subsequent death of the neutrophil [14]. Electron microscopy is used in many studies to distinguish between these two phenotypes of NETs [11,13]. However, electron microscopy analysis is a costly and time-consuming method.

In previous studies, we have shown that *S. suis* is entrapped in NETs in the CSF *in vivo* [15] and induces vital and suicidal NETs *in vitro* [16]. Nevertheless, without treatment, *S. suis* can lead to the death of the host [17,18]. This study aimed to investigate the host-pathogen interaction between *S. suis* and neutrophils in the CSF compartment with regard to alive and impaired NET-releasing neutrophils, using a method that is easy to use and less costly. For this purpose, we used an *in vitro* model of the porcine BCSFB (adapted from Meurer et al.) [19], which utilizes a porcine choroid plexus epithelial cell line (PCP-R) [20,21] in a cell culture filter system. After infection with *S. suis*, neutrophils were added and analyzed for NET-formation by confocal fluorescence microscopy.

2 Material and Methods

2.1 Bacterial Strain and Growth Conditions

Streptococcus suis strain 10 (*S. suis* 10) is a virulent wild-type serotype 2 strain that has been used in various *in vitro* studies before [15,19,22]. This strain was kindly provided by Hilde Smith (Wageningen, GE, The Netherlands) [23]. For the assays, working cryostocks were generated. *S. suis* 10 were cultivated on Columbia Agar with 7% sheep blood (Thermo Fisher Scientific, Waltham, MA, USA; PB5008A), and one colony was afterwards grown in Todd Hewitt Broth medium (THB) (Thermo Fisher Scientific, Waltham, MA, USA; 249240) at 37°C for 20 h. From this overnight culture, a growth curve was conducted until the late exponential growth phase (Optical density $(OD)_{600nm}$ = 0.85 ± 0.02). The OD was measured with a spectrophotometer (Cole-Parmer (former Jenway) Model 6300, St. Neots, England). To prepare the working cryostocks, the culture was mixed with glycerol (final concentration of 15%), and aliquots were frozen at −80°C. To determine the colony-forming units per mL (CFU/mL), serial dilutions were plated on blood agar plates and then quantified. Each cryostock was used only once.

2.2 Collection of Porcine Blood

Blood was collected from healthy pigs (total n = 3; male = 1; female = 2) that were euthanized due to other reasons. Euthanasia of pigs was approved and registered by the local Animal Welfare Officer at the University of Veterinary Medicine Hannover, Germany, in accordance with the German Animal Welfare Law under the following number: TiHo-T-2024-16. Since the study was conducted over an extended period, new registrations had to be made regularly in accordance with legal requirements, which then generated a new number: TiHo-T-2025-2. A registration number does not solely represent the registration of pigs used exclusively in this project; rather, it covers a variety of projects from the Institute of Biochemistry, where material from healthy pigs was obtained through euthanasia for scientific purposes. Fresh blood was collected in S-Monovette® Lithium-Heparin 9 mL tubes (Sarstedt, Nümbrecht, Germany) from the dead animals.

Method of euthanasia: The pigs were anesthetized with azaperone (2 mg kg^{-1} body weight (BW), Stresnil ad us. vet., Elanco Tiergesundheit AG, Basel, Switzerland) and ketamine-hydrochloride (20 mg kg^{-1} BW, Ursotamin, 100 mg mL^{-1}, Serumwerk Bernburg AG, Bernburg, Germany) intramuscularly. The depth of anesthesia was proven by observation of a trained veterinarian. The pigs were euthanized intravenously with T 61® (3–4 mL/50 kg BW, Intervet Deutschland GmbH, Unterschleißheim, Germany) during anesthesia. The death of the pig was determined by a trained veterinarian. The procedure of euthanasia followed the recommendations for euthanasia of experimental animals [24].

In addition, blood was collected in 50 mL lithium-heparin tubes at the slaughterhouse from healthy pigs (total n = 15; male = 7; female = 8) during the slaughter process. The slaughter of the pigs at the slaughterhouse was carried out by bleeding in accordance with the applicable laws in Germany. For this, the animals were first stunned using electricity, and the sampling of blood complied with relevant regulations. The blood was used within one hour after blood collection for neutrophil isolation. The use of blood from the slaughterhouse was reported to the animal welfare officer of the University of Veterinary Medicine Hannover, Germany, and registered under the number TVT-2025-P-31 in connection with Laura Schaltz's PhD project.

All pigs (German Landrace) included in this study came from conventional herds and included females and males. The age of the pigs was between 6–7 months. To ensure statistical independence, only one neutrophil isolation from one pig was used for each experiment. Each neutrophil isolation, therefore, was considered to be an experimental unit. As we used blood only in *in vitro* assays, no exclusion criteria were set during the *in vitro* experiment. The blood donors were only included if they were clinically healthy. The blood donors were not excluded after blood donation. They were randomly selected without specific guidance, and confounders were not controlled. As no groups were compared in this study, blinding of the experimenter was not necessary. The following parameters were assessed: the number of isolated neutrophils per mL and the NET formation capacity of isolated neutrophils.

2.3 Isolation of Porcine Neutrophils

The isolation of porcine neutrophils was performed using density gradient centrifugation with BioColl separation solution (Bio&SELL, Feucht, Germany; L6115) and lysis steps of erythrocytes. Therefore, blood was mixed with 1 volume of Lipopolysaccharides (LPS)-free PBS (Sigma-Aldrich, Merck KGaA, Darmstadt, Germany). In a 50 mL conical tube, 12 mL of Biocoll Separation Solution (density: 1.077 g/mL) was added to the bottom. Then, 12 mL of the blood-PBS mixture was carefully layered on top of the Biocoll solution. This gradient was centrifuged at 400× *g* for 20 min at 20°C, without applying the rotor brake after centrifugation. The supernatant above the red bottom layer was removed, and the red layer was resuspended in 8 mL of ice-cold 0.2% sodium chloride in the same conical tube for erythrocyte lysis. The tube was inverted

for 30 s, after which 8 mL of ice-cold 1.6% sodium chloride was added. The cell suspension was then centrifuged at 250× *g* for 7 min at 4°C, this time using the rotor brake. The supernatant was discarded, and the erythrocyte lysis procedure was repeated up to two more times until the remaining cell pellet appeared white. The cell number was adjusted to 2×10^5 cells/well (NET induction assay) or 8×10^5 cells/mL (transmigration assay). The neutrophils were resuspended in RPMI medium 1640 (Gibco, Thermo Fisher Scientific, Eggenstein-Leopoldshafen, Germany; 11835-063) (NET induction assay) or 1% fetal calf serum (FCS) (Biochrom, Merck, Darmstadt, Germany; S0615) cell culture medium (transmigration assay).

2.4 NET Induction Assay

For the assay, 8 mm coverslips were coated with poly-L-lysine in 48-well plates according to the manufacturer's description (0.001% solution (Sigma Aldrich, Merck, Darmstadt, Germany; P4707) for 20 min and washed three times with LPS-free 1× PBS. 2×10^5 cells/100 µL were seeded on each coverslip. The final volume in each well is 200 µL. For the negative control, neutrophils were treated with Rosewell Park Memorial Institute medium 1640 (RPMI). For positive control, 10 mM methyl-β-cyclodextrin (CD) (Sigma Aldrich, C4555-1G) was added. Treatment with 1% FCS cell culture medium was also administered to determine whether this influences NET-formation. The neutrophils were also infected with *S. suis* 10 with a multiplicity of infection (MOI) = 2. To rule out a possible influence of interleukin-8 (R&D Systems, Wiesbaden, Germany; 535-IN-025/CF), 20 ng/200 µL IL-8 was tested in the assay (concentration adjusted to the transmigration assay). The cells were incubated for two and four hours at 37°C with 5% CO_2. Before and after incubation, the plates were centrifuged (250× *g*, 5 min). Afterwards, the cells were stained immediately.

2.5 Cell Culture and Transmigration Assay

The cell culture model with porcine choroid plexus epithelial cells was adapted from Meurer et al. [19,21]. This cell line is not commercially available and was provided by the authors, Schwerk and Schroten [20]. The cells are regularly tested for mycoplasma contamination every three months. All experiments were conducted with mycoplasma-negative cells. The experiments were conducted in 24-well plates with poly-L-lysine-coated 12 mm coverslips. The filters were incubated in 1% FCS (Biochrom, Merck, Darmstadt, Germany; S0615) medium and infected with *S. suis* 10 with a MOI of 5. For the transmigration assays, 8×10^5 neutrophils/mL were added to the upper compartment and incubated for four hours at 37°C with 5% CO_2. To attract the neutrophils, 100 ng recombinant porcine interleukin-8 (R&D Systems, Wiesbaden, Germany; 535-IN-025/CF) were added to the lower compartment (1000 µL). The CFU/mL was determined in the lower compartment by plating serial dilutions on blood agar plates and then quantified. As a negative control, uninfected filters were used. As a control experiment, CD (final concentration 10 mM) was added to the lower compartment (Fig. A1). To determine cell layer integrity, the transepithelial electrical resistance (TEER) was measured with a Millicell® ERS-2 (Millipore, Billerica, MA, USA) voltmeter before and after the incubation and calculated for each filter. The TEER of each filter was calculated by multiplying the resistance value (Ω) by the area of the membrane (cm^2) [25]. The plates were centrifuged (250× *g*, 10 min) and immediately stained as described below.

2.6 NET Staining

For the staining of impaired cells, Live-or-Dye NucFix™ Red Staining Kit (Live-or-Dye) (Biotium, Fremont, CA, USA; 32010-T) was used. The stock was dissolved in anhydrous Dimethyl sulfoxide (DMSO) in accordance with the manufacturer's description (stock 1000× in DMSO). In each well, 200 µL Live-or-Dye diluted 1:2000 in phosphate-buffered saline (1× PBS, pH 7.4) was added and incubated for 30 min at 4°C in

the dark. After centrifugation (250× *g*, 5 min), the wells were washed with 1× PBS and fixed afterwards with 4% paraformaldehyde (PFA) (Science Services, E15710, Munich, Germany). The plates were stored at 4°C in 1× PBS and wrapped with parafilm. NETs were stained as previously described [15]. Briefly, a mouse monoclonal antibody (IgG2a) against DNA/histone 1 complexes (DNA/histone 1) (Millipore, Billerica, MA, USA, MAB3864, 0.55 mg/mL, 1:909) was used as the primary antibody and incubated for one hour at room temperature in the dark. For the isotype control, IgG2a from murine myeloma (Sigma, M5409, 0.2 mg/mL, 1:364) was added. As a secondary antibody, goat-anti-mouse IgG Alexa Fluor 488Plus (Invitrogen, Carlsbad, CA, USA, A32723, 2 mg/mL, 1:500) was used for one hour at room temperature in the dark. To stain the nucleus of the cells, aqueous Hoechst 33342 (Sigma, 14533, 50 mg/mL, 1:1000) was used for 10 min at room temperature in the dark. The coverslips were embedded on glass slides in Prolong Gold (Invitrogen, P36930) for the NET induction assays or Prolong Diamond (Invitrogen, P36970) for the transmigration assays and dried overnight at room temperature. The slides were stored at 4°C until microscopy analysis.

2.7 Confocal Microscopy

Microscopy images were recorded using a Leica (Wetzlar, Germany) TCS SP5 AOBS confocal inverted-base fluorescence microscope with a HCX PL APO lambda blue 40×/1.25 oil immersion objective and Argon (488 nm), 405 nm, and 561 nm lasers. The settings were adjusted with control preparations using the isotype control to exclude unspecific signals of first and secondary antibodies, as well as autofluorescence.

2.8 NET Quantification

For the NET induction assay, six images were randomly taken from each sample on two coverslips. The cells in the picture were counted manually with ImageJ software (National Institute of Health, USA, version v1.54g). The conditions under which a cell is considered positive for NETs are previously described [16], with the following changes: In each sample, a minimum of 250 cells were counted. A neutrophil was counted as positive if an evident offshoot of DNA was visible, or if at least two of the following criteria were found: enlarged nucleus, decondensed nucleus, or blurry rim. Additionally, there is a differentiation between NET positive impaired (Live-or-Dye positive) and NET positive alive (Live-or-Dye negative). The average from all six images taken in one experiment was calculated for each sample to calculate the statistics. For the transmigration assay, 13 images were taken in a specific pattern from the uninfected and *S. suis* 10 infected cells to achieve a sufficiently high cell number for counting. The evaluation was performed as in the NET induction assay.

2.9 Flow Cytometry

2×10^5/500 µL isolated porcine neutrophils were incubated in RPMI 1640 medium with or without *S. suis* 10 (MOI of 2) for two and four hours at 37°C with 5% CO_2. During the last 30 min of the incubation period, 2.5 µL Live-or-Dye NucFix™ Red Staining Kit (Live-or-Dye) (1:2000) and 10 µL DCF (2′,7′-Dichlorodihydrofluorescein diacetate; Sigma Aldrich, Merck, Darmstadt, Germany; D6883) (1:1000), diluted in RPMI medium 1640, were added (final concentration 10 mM). Flow cytometry was performed using an Attune NxT Flow Cytometer (Thermo Fisher Scientific, Eggenstein-Leopoldshafen, Germany). Cells were stained with DCF to detect intracellular reactive oxygen species (ROS) and with the Live-or-Dye NucFix™ Red Staining Kit to assess cell viability. DCF fluorescence was excited with the blue laser (488 nm) and detected in the corresponding emission channel at 530 nm (BL1). The Live-or-Dye was excited with the yellow laser (561 nm), and its emission was detected at 620 nm (YL1). Samples were measured at a flow rate of 100 µL/min with a total acquisition volume of 100 µL per sample. Forward scatter (FSC) and side scatter (SSC) parameters

were used to identify the main cell population. Control samples included untreated live cells, heat-killed cells (70°C for 10 min), and a 1:2 mixture of live and heat-killed cells to verify viability discrimination. For fluorescence compensation and gate setting, single-stained controls for each dye as well as double-stained samples were prepared and measured. The gating strategy included the determination of singlets of all cells, followed by the mean green fluorescence intensity of all cells (X-Mean of BL-1) as a relative measurement of ROS production. Data was analyzed with FlowJoTM11.1.1 software (Ashland, OR, USA).

2.10 Statistical Analysis

The data were analyzed with Excel 365 (version 2508, Microsoft). The statistical evaluation was made with GrapPad Prism software (San Diego, CA, USA, version 10.4.1). Normal distribution of data was verified by the Kolmogorov–Smirnov normality test prior to statistical analysis. Data was analyzed with one-tailed paired or unpaired Student's *t*-test and presented with mean ± SD. The statistical tests used are indicated in the figure legends. The Pearson correlation coefficient (r) was used to determine the linear relationship between different variables. A heatmap was created to represent the correlation matrix. Red shades ($r < 0$) represent negative correlations and blue shades ($r > 0$) represent positive correlations. The *p*-values were defined as follows: $^{*}p < 0.05$, $^{**}p < 0.01$, $^{***}p < 0.001$, $^{****}p < 0.0001$.

3 Results

3.1 Indication of High Numbers of NET-Activated Alive Cells after Two Hours of S. suis Infection in Porcine Neutrophils

S. suis induces NET-formation in neutrophils *in vivo* and *in vitro* [15,16,19]. However, as *S. suis* possesses mechanisms to evade this defense mechanism [9,26] and survives in the host, the question raises if NET-activated neutrophils die during this host-pathogen interaction. For this reason, we have established a staining method with Live-or-Dye NucFix™ Red Staining Kit (Live-or-Dye) that can be used to stain alive and impaired cells. In combination with established NET markers, it is possible to differentiate between alive and impaired cells forming NETs after PFA fixation by confocal microscopy (Fig. 1A). With this method, we were able to stain NETs induced by *S. suis* (Fig. 1B,C). Both NET-negative and -positive (NET-activated) cells can be detected. Therefore, a distinction can be made between NET-positive alive and impaired neutrophils. To differentiate between them, all NET-positive and NET-negative cells are counted, as well as cells that are NET-positive and stained with Live-or-Dye (Fig. 2A–C).

The NET induction assay showed that *S. suis* leads to an overall increase in NET-formation (Fig. 2A). Furthermore, fewer NETs can be detected if neutrophils are infected with *S. suis* in the presence of FCS-containing medium. There are only minor differences between the total number of impaired cells and impaired cells that are NET-positive (Fig. 2B,C). From this, it can be deduced that most impaired neutrophils form NETs to counteract *S. suis*. In the overall comparison, after two hours of infection with *S. suis*, there are more NET-activated and alive neutrophils than impaired ones (Fig. 2D). This phenotype is also identified if neutrophils are infected with *S. suis* in the presence of FCS-containing medium. These data indicate that the combination of Live-or-Dye staining with NET markers enables the quantification of NET-activated impaired and alive cells.

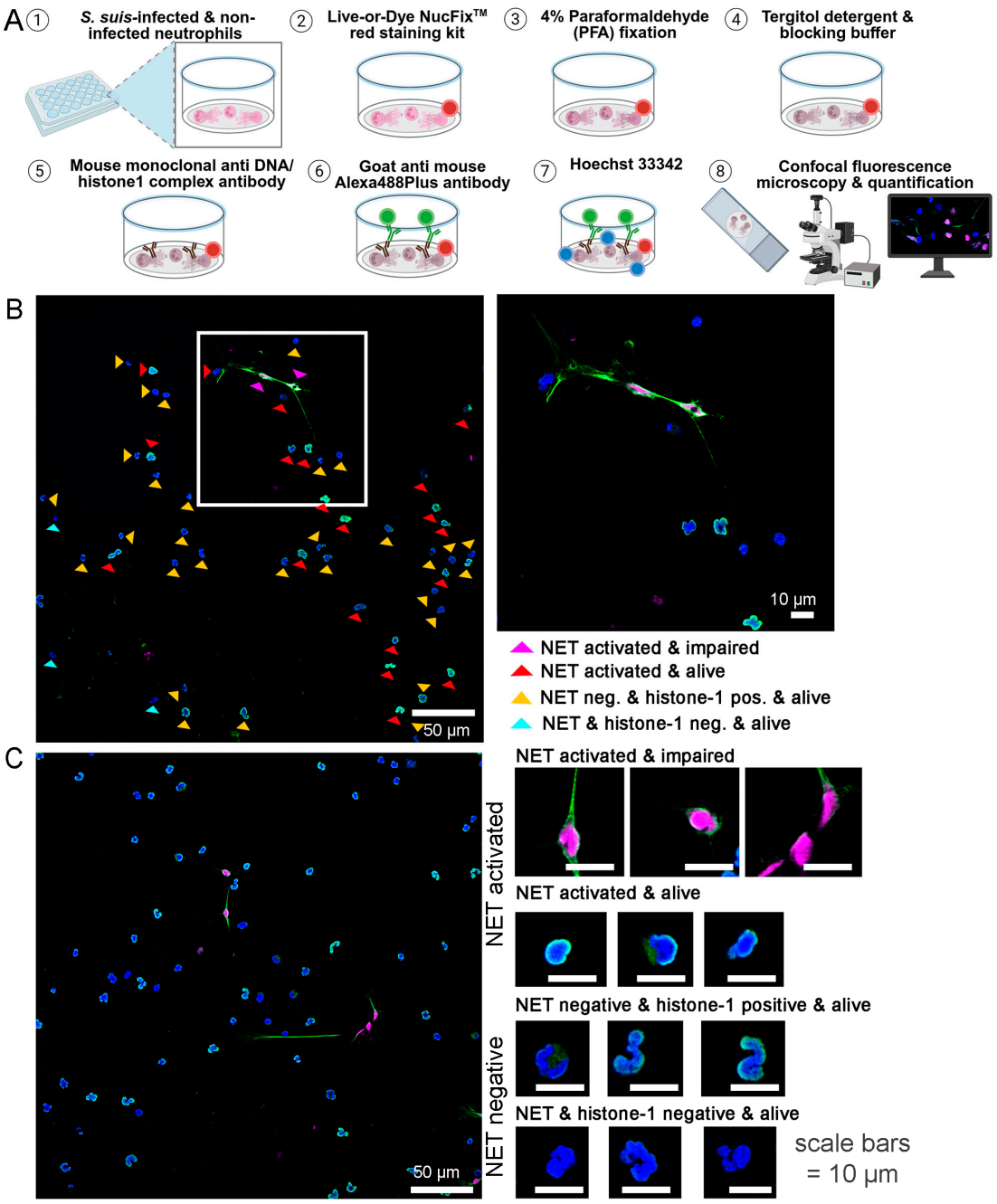

Figure 1: The combination of Live-or-Dye and NET markers enables the differentiation between alive and impaired cells: (**A**) A new protocol of NET staining was established to combine three markers: Live-or-Dye as a cell membrane impermeable dye for impaired cell nuclei; mouse monoclonal anti-DNA/Histone1 (DNA/Histone1) antibody as a specific primary antibody for NETs; Hoechst 33342 as a cell membrane permeable dye for nuclear staining of DNA; (**B**) Example images from confocal immunofluorescence microscopy of neutrophils incubated with *S. suis* for two hours (blue = DNA (Hoechst 33342); green = NET marker (DNA/Histone1), magenta = impaired cell (Live-or-Dye). Neutrophils that have an altered cell nucleus and are stained with DNA/Histone1 and Live-or-Dye (=magenta) are counted as NET-positive and impaired. Cells with an altered cell nucleus and additionally stained with DNA/Histone1 (=green) can be identified as NET-positive and alive. Cells with an unchanged cell nucleus and stained with DNA/Histone1 (=green) can be identified as NET-negative and alive. Cells that are only stained with Hoechst 33342 (=blue) can be detected as NET-negative and alive.

An example counting for different NET phenotypes is included. To differentiate between the different NET phenotypes, cells were counted in an overlay image. In addition, cells were counted in the Live-or-Dye channel and compared with the NET staining. If both were positive, these cells were classified as NET-positive and impaired (magenta arrow heads). The zoom image shows impaired cells that have been stained with Live-or-Dye in the area of the cell nucleus and with DNA/Histone1 in the area of the fibers, allowing clear differentiation between NET-positive impaired and alive cells; (**C**) In this example image, three neutrophils were enlarged for each NET phenotype. Fig. 1A was created in BioRender. de Buhr (2026) https://BioRender.com/4z3vtdq.

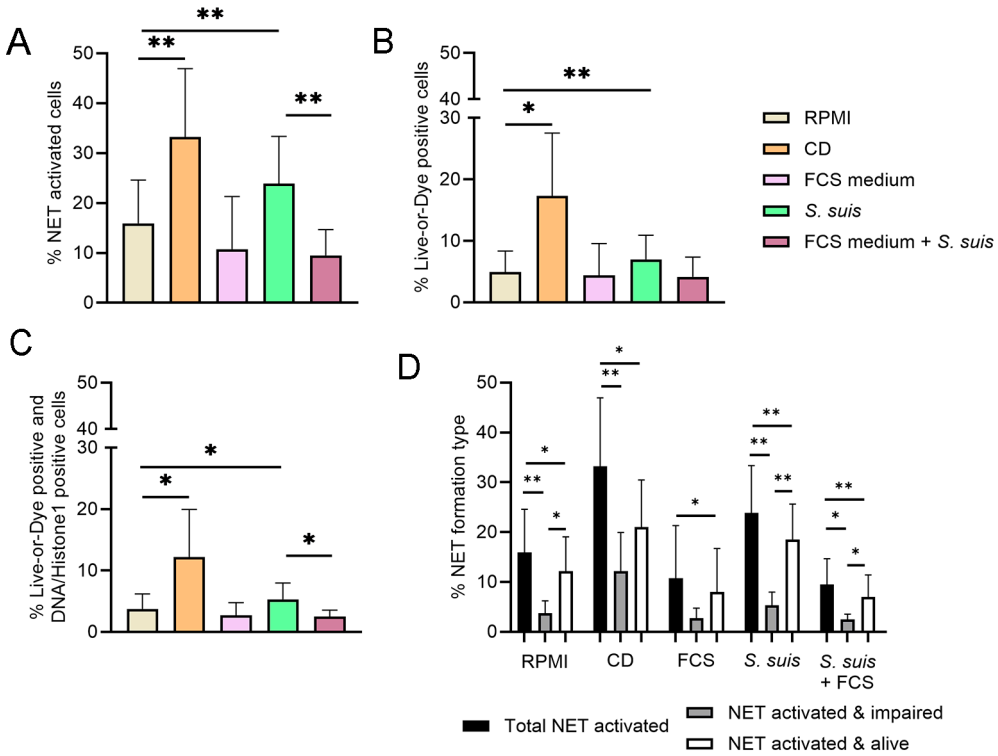

Figure 2: Analysis of neutrophil viability and NET formation under various stimulation conditions: (**A**–**D**) Neutrophils were incubated for two hours in the presence of different media: RPMI (Rosewell Park Memorial Institute Medium) was used as a negative control, and CD (methyl-β-cyclodextrin) as a positive control. Data are shown as the mean ± SD from $n = 5$ independent experiments with duplicates in each technical run. Statistical analysis: one-tailed paired Student's t-tests ($^{*}p < 0.05$, $^{**}p < 0.01$). (**A**) Quantification of NET-activated cells. (**B**) Quantification of neutrophils positive for Live-or-Dye. This quantification shows all impaired cells in the different media (both NET-positive and NET-negative). (**C**) Quantification of neutrophils that were positive for Live-or-Dye and DNA/Histone1. This variant shows all impaired cells in the different media that are in addition NET-positive. (**D**) Comparative representation of total NET-formation (all features indicative of NETs), NET-positive and impaired cells (DNA/Histone 1 and Live-or-Dye positive), and NET-positive and alive cells (only DNA/Histone 1 positive).

3.2 Indications That CFU/mL May Influence the Increased Number of NET-Activated and Impaired Porcine Neutrophils after Transmigration

In the next step, we used an *in vitro* model of the BCSFB [15,19] and analyzed transmigrated neutrophils after *S. suis* infection for the NETs activation and whether the neutrophils are alive or impaired (Fig. 3A). Therefore, neutrophils were stained with the established Live-or-Dye protocol (Fig. 1) after transmigration through the BCSFB barrier in the *S. suis* infected CSF compartment and compared with uninfected samples

(Fig. 3B). *S. suis* causes more neutrophils to transmigrate through the BCSFB than in uninfected wells. Neutrophils do not migrate evenly through the BCSFB and seem to form small groups after transmigration. When the chemical NET inducer CD is added as a stimulus into the CSF compartment, the barrier integrity drops (Fig. A1A), and only a very minimal number of neutrophils transmigrate (Fig. A1B,C). In comparison to an uninfected sample, *S. suis* leads to increased NET-formation (Fig. 3C). Only a small proportion of uninfected neutrophils form NETs, and these are mainly alive. 46.9% (SD ± 12.9%) of neutrophils that transmigrated into the *S. suis*-infected CSF compartment form NETs. Comparing the NET-activated cells, the neutrophils are significantly more NET-activated and impaired after four hours of transmigration in the presence of *S. suis*. However, a small neutrophil population (9.8% SD ± 8.7%) remains NET-activated and alive. Nevertheless, *S. suis* grows in the CSF compartment (Fig. 3D). It can be deduced that the more neutrophils are NET activated, the more neutrophils are impaired (Fig. 3E). This can also be linked to the CFU/mL. The more neutrophils are NET-activated and impaired, the higher the CFU/mL after one hour. Conversely, the more neutrophils are NET activated and alive, the lower the CFU/mL after one and five hours. These data indicate that *S. suis* leads to increased NETosis with high numbers of impaired NET-activated neutrophils and lower numbers of alive NET-activated neutrophils, which could still perform phagocytosis. In addition, there is evidence to support the assumption that the number of alive or impaired neutrophils that are NET activated depends on the CFU/mL.

To identify if the observed phenotype of increased impaired NET-releasing neutrophils is due to the transmigration and/or factors released by the PCP-R cells, we conducted NET assays without transmigration, but in the presence of substances present in the BCSFB model. The two cell culture additives (IL-8 and FCS) do not induce NETs. Overall, without transmigration, there is a higher number of NET positive cells (NET activated) if *S. suis* is present (Fig. 4A,B). The co-incubation with the cell culture additives and *S. suis* does not significantly change the NET release. Presumably, *S. suis* is the main trigger for NET formation in cell culture, with less IL-8 and FCS medium. As in the cell culture experiments, after four hours, most neutrophils are impaired and NET activated in the presence of *S. suis* (Fig. 4C,D). When all stimuli are present, the highest number of impaired NET-activated neutrophils is observed, but there is no significant difference compared to the others. The CFU/mL is higher in this NET induction assay after four hours (Fig. 4E) compared to the cell culture experiment (Fig. 3D).

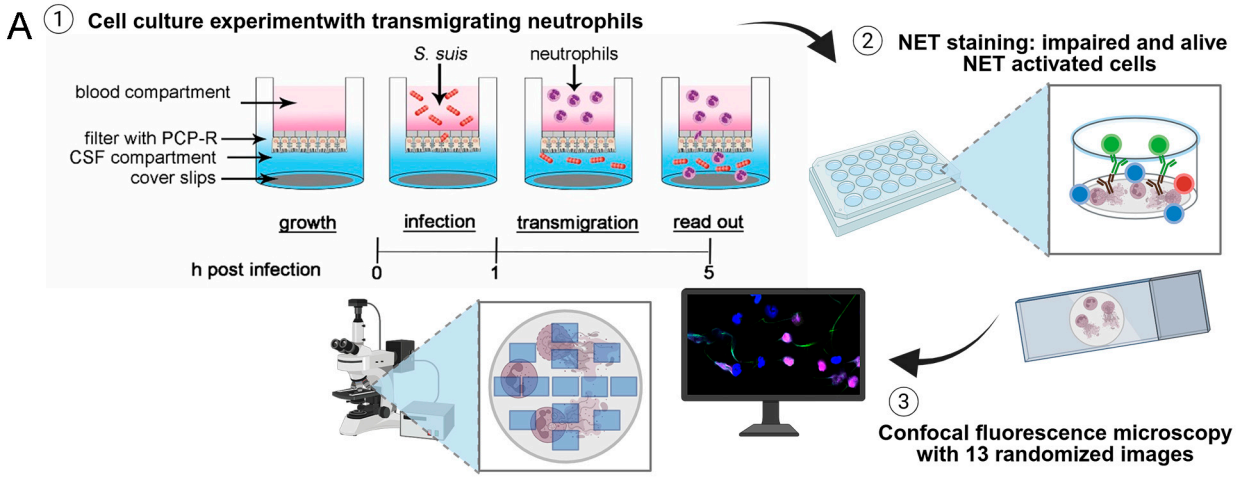

Figure 3: *Cont.*

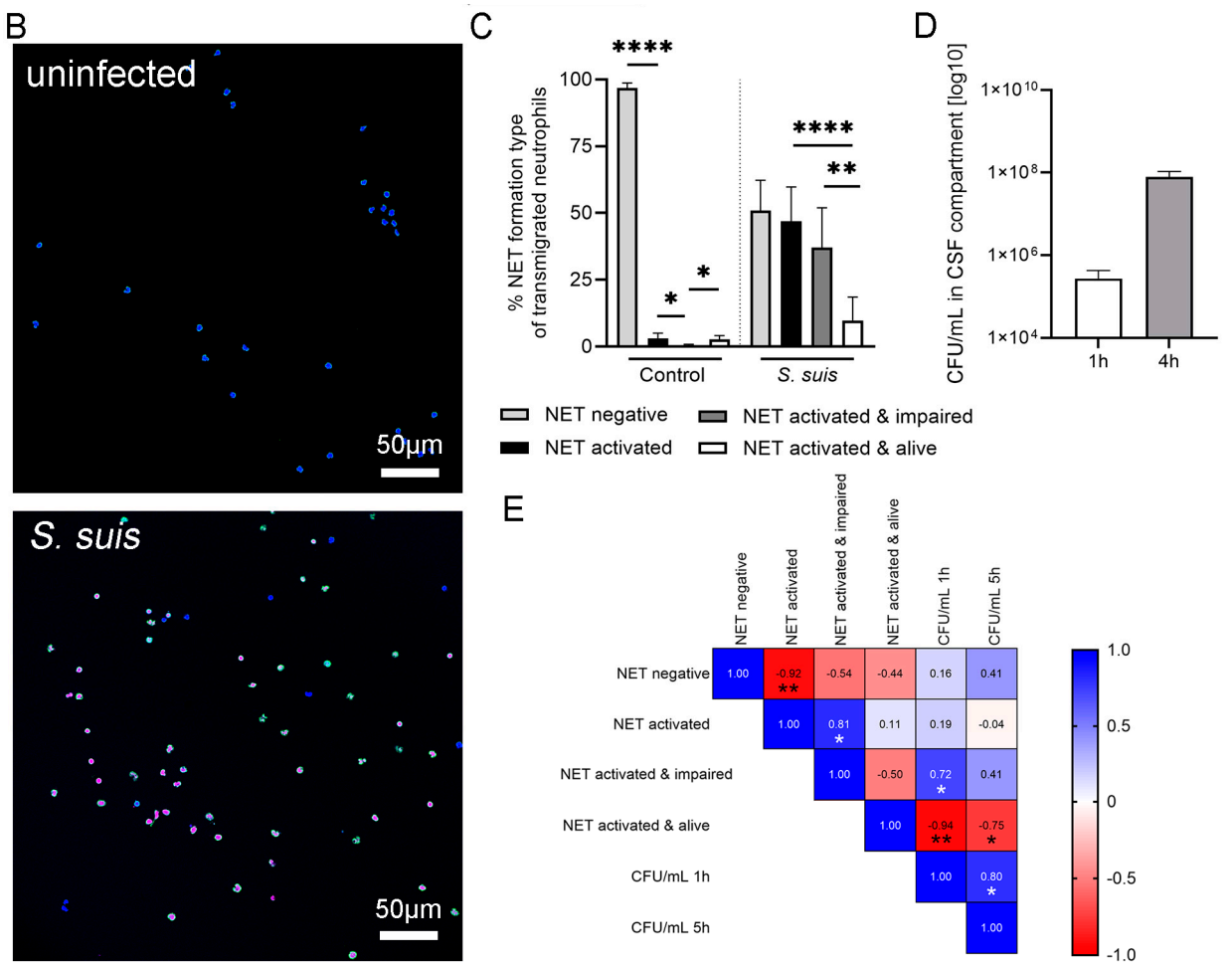

Figure 3: *S. suis* has an impact on transmigrated neutrophils through a barrier of porcine plexus epithelial cells, depending on the CFU/mL: (**A**) The *in vitro* model of the BCSFB is infected with *S. suis* for one hour in the "blood" compartment; afterwards, neutrophils are added for four hours to the "blood" compartment. Transmigrated neutrophils are evaluated for their NET phenotype on 13 images using a confocal fluorescence microscope. The number of images is generated in a specific pattern to quantify an appropriate number of cells. (**B**) Representative images of transmigrated neutrophils with and without *S. suis* after four hours. Blue = DNA (Hoechst 33342), green = NET marker (DNA/Histone1), magenta = impaired cells (Live-or-Dye). (**C**) Compared to uninfected neutrophils, a *S. suis* infection leads to increased NET-formation. There is a significant difference between NET-positive impaired and alive cells. While the uninfected cells are mainly alive, the *S. suis*-infected neutrophils are mostly impaired. Data shown as mean ± SD, $n = 5$ independent experiments. Statistical analysis: one-tailed unpaired t tests ($^{*}p < 0.05$, $^{**}p < 0.01$, $^{****}p < 0.0001$). (**D**) The CFU/mL increases over time in the CSF compartment. The scale of the y-axis is set to log10. (**E**) Heatmap of a Pearson correlation from the transmigration assay, which represents the relation between NET-negative and NET-positive as well as impaired and alive cells in correlation with the CFU/mL. Statistical analysis: Pearson correlation ($^{*}p < 0.05$, $^{**}p < 0.01$); Red shades ($r < 0$) represent negative correlations and blue shades ($r > 0$) represent positive correlations. Fig. 3A was created in BioRender. de Buhr (2026) https://BioRender.com/0akz6ek.

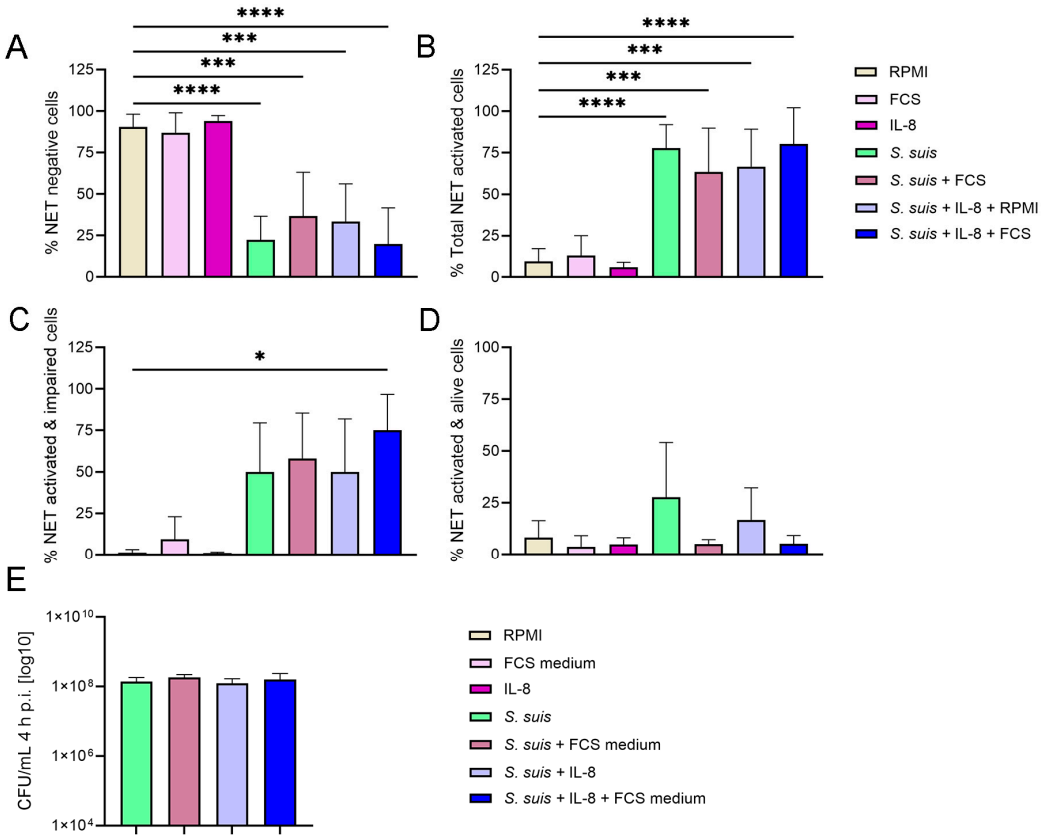

Figure 4: *S. suis* has an impact on the membrane integrity of NET-activated neutrophils after four hours: (**A**,**B**) Isolated porcine neutrophils were incubated for four hours with various media and stimuli: RPMI as a negative control and *S. suis* as a positive control. In the absence of *S. suis*, most neutrophils are NET negative, whereas *S. suis* induces NETs. (**C**,**D**) Most of the *S. suis* NET-activated cells are impaired. *S. suis*, in combination with the cell culture additives, leads to the highest number of impaired neutrophils, while *S. suis* alone has the most alive cells. (**E**) The CFU/mL is identical in all four infection groups. The scale of the *y*-axis is set to log10. Data shown in all graphs as mean ± SD, $n = 4$ independent experiments. Statistical analysis: ANOVA, followed by a multiple comparisons test (Dunnett multiple comparisons test, $^{*}p < 0.05$, $^{***}p < 0.001$, $^{****}p < 0.0001$).

Finally, we analyzed whether neutrophils (alive or impaired) remain capable of executing another defense mechanism: ROS production. To assess this, we performed flow cytometric analysis to evaluate cell viability and the release of ROS (Fig. 5). The purity of the isolated neutrophils was 90.4% ± SD 4.5% (Fig. 5C). Since *S. suis* infection causes neutrophils to shift out of the neutrophil gate (Fig. 5D), by loosing size and granularity, we decided to analyze all singlets in the assays (Fig. 5E). The data reveal that after two hours of infection, the majority of *S. suis*-infected neutrophils remain alive, whereas after four hours, there is an increase in the number of Live-or-Dye positive cells (impaired cells) (Fig. 5G). Consistent with this, ROS release is increased after two hours of *S. suis* infection but significantly decreases after four hours compared to an uninfected control (Fig. 5H). Interestingly, ROS release was observed in both alive and Live-or-Dye positive (impaired) cells. In the alive neutrophil population, *S. suis*-infected neutrophils released significantly higher amounts of ROS after both two and four hours (Fig. 5J). In contrast, in the impaired neutrophil population, *S. suis*-infected neutrophils released significantly higher amounts of ROS only after two hours (Fig. 5K).

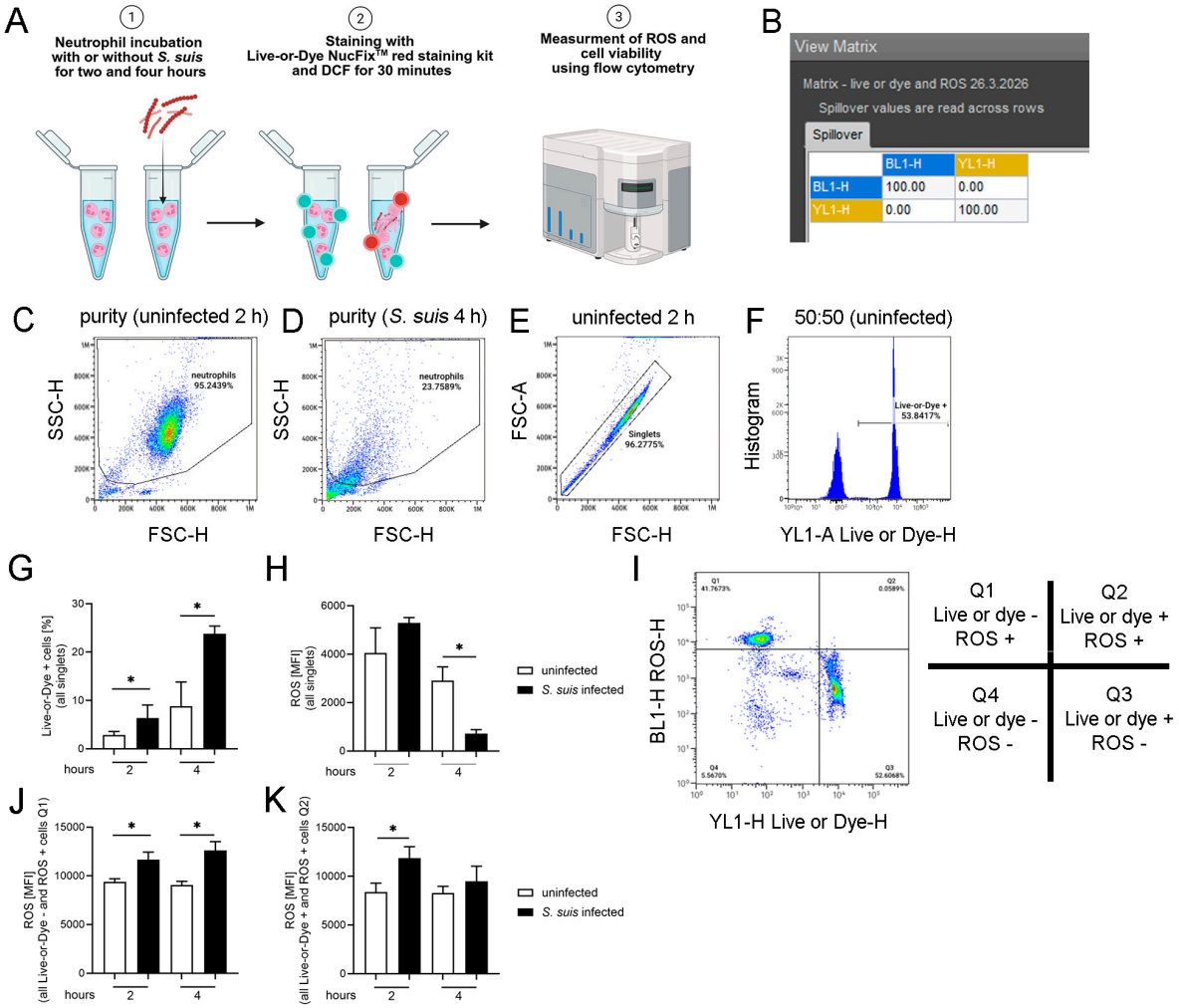

Figure 5: Live-or-Dye positive and negative cells produce ROS during *S. suis* infection: (**A**) To show cell viability and ROS production, uninfected and *S. suis*-infected neutrophils were stained with Live-or-Dye as a cell death marker and 2′,7′-Dichlorodihydrofluorescein diacetate (DCF) to determine ROS production after two and four hours of incubation time. DCF is cell-permeable, and its fluorescence is activated by oxidation with ROS. The results were analyzed by flow cytometry and are presented with the gating strategy and example plots. (**B**) Compensation was done to exclude the spillover of signal during the measurement. (**C**,**D**) Whereas a gate for neutrophils in uninfected cells is possible to be set, after *S. suis* infection, all neutrophils shift out of the uninfected neutrophil gate. Therefore, in the analysis, no neutrophil gate was set. (**E**) Based on FSC-A and FSC-H, singlets were gated from all cells. (**F**) The Live-or-Dye staining was gated with controls containing an equal amount of alive and heat killed neutrophils (1:2 = 50:50). (**G**) Live-or-Dye positive cells were analyzed at the two timepoints and compared between uninfected and infected samples. (**H**) The mean fluorescence intensity (MFI) of ROS production was analyzed at the two timepoints and compared between uninfected and infected samples. (**I**) Single cells were analyzed in a two-parameter dot plot with quadrant gating to distinguish the different neutrophil populations in a control containing an equal amount of alive and heat-killed neutrophils; Q1 = alive & ROS positive, Q2 = impaired & ROS positive, Q3 = impaired & ROS negative, Q4 = alive & ROS negative. (**J**) The ROS MFI of all cells negative for Live-or-Dye [Q1] was compared between groups. (**K**) The ROS MFI of all cells positive for Live-or-Dye [Q2] was compared between groups. Data is presented as the mean ± SD (n = 3 independent experiments). Statistical analysis: paired Student's t-test (*$p < 0.05$). Fig. 5A was created in BioRender. de Buhr (2026) https://BioRender.com/d1b6p2h.

4 Discussion

The first description of NETs was published more than 20 years ago [7]. The first description of vital NETosis following *Staphylococcus aureus* infection was made over 15 years ago [27] and has been widely discussed [14,28]. Nonetheless, it is still not understood whether a stimulus in neutrophils can trigger only vital NETosis or also suicidal NETosis, or if these are two sequential mechanisms. Wang et al. discussed in one recent review that the investigation of the mechanisms behind NET formation is still in early stages, focusing on the induction of NETs by various microbes through suicidal and vital NETosis. They claimed that an understanding of the differences in NET-formation under physiological and pathological conditions, as well as the variations in NET components, is crucial for identifying new targets to regulate NETs in diseases [29].

Already in 2015, a method to quantify vital and suicidal NETosis using multispectral imaging flow cytometry was published [30]. Nevertheless, the study lacked validation using, for example, electron microscopy to truly determine whether it is possible with this technique to differentiate between vital and suicidal NETs as described in the original study [27]. Furthermore, there have been ongoing discussions about this method, as it can only be performed by laboratories with specialized expertise and highly specific equipment [31]. In 2016, it was suggested that this method could be an excellent quantification technique if it were regularly used [32]. However, unfortunately, ten years after its publication, there are only a few studies that have used or attempted to improve this method [33–36]. Moreover, to the best of our knowledge, it has only been used once more to differentiate between vital and suicidal NETosis [37].

Suicidal NETosis leads to decondensation and disruption of the neutrophil membrane [27]. Vital NETosis involves the formation of vesicles released via nuclear budding [14], and the neutrophil membrane remains intact. In fact, our group has demonstrated, by using electron microscopy, vital NET-formation in porcine neutrophils after just a 30-min infection with *S. suis* [16]. Here we investigated later time-points with two and four hours, without and with transmigration of the neutrophils, and with different combinations of stimuli (Figs. 2–4).

We used the combined staining of DNA/histone 1 complexes and Live-or-Dye NucFix™ Red staining. Live-or-Dye NucFix™ Red only stains cells with permeable membranes and remains stable during fixation and permeabilization. The newly established protocol can be used to differentiate between alive and impaired NET-activated neutrophils. Consequently, this method allows for the identification of NETs but does not permit discrimination between different forms of NETosis (e.g., vital versus suicidal) or the specific pathways involved. However, in combination with confocal immunofluorescence microscopy and manual counting, we quantified alive and impaired NET-activated neutrophils (Figs. 1–4). Since verification via electron microscopy was not performed in our study, we deliberately opted not to use the terms “vital” and “suicidal” as coined by Fuchs et al. 2007 [27]. Instead, we categorize the identified cells based on staining: those with loss of membrane integrity and positive signal of Live-or-Dye NucFix™ Red staining as “impaired” neutrophils, and those not detected by this dye are termed as “alive”. As expected, we found that alive neutrophils were still able to produce ROS, suggesting that cell function is preserved, especially in the presence of *S. suis* (Fig. 5J). Several studies have reported an increase in ROS released by neutrophils after *S. suis* infection [26]. However, results varied depending on the donor species of the neutrophils (human, mouse, pig), the strain of *S. suis* used, the incubation time, and the assay set-up [38–40]. Therefore, it can be hypothesized that the alive neutrophils are capable of continuing to form ROS-dependent NETs.

Live-or-Dye dyes are designed to primarily stain cells with severely damaged membranes, such as dead or highly compromised/impaired cells. We chose to use the term “impaired” because neutrophils that tested positive with Live-or-Dye staining were still able to produce ROS in the presence of *S. suis* at specific fixed time points (Fig. 5K). This observation suggests that Live-or-Dye may not exclusively label fully

dead cells, but also cells in a transitional state in which membrane integrity is progressively compromised. In such cases, the dye can enter while neutrophils may still retain functional activity. This aligns with the process of NETosis, during which pore formation occurs and membrane permeability increases already early in the process [41,42]. Accordingly, these neutrophils may be interpreted as being in a transient stage rather than fully dead. In addition, it is noted that neutrophils can affect their surroundings after death and that the process of neutrophil death is highly variable [43]. Recently, it was shown that neutrophils can undergo "death" twice. After a stimulus triggers apoptotic signaling and progression towards apoptosis, pores can be formed by the protein gasdermin E. This leads to a calcium influx and activation of Peptidyl arginine deiminase 4 (PAD4), resulting in NETosis [44,45]. The involvement of gasdermin E in NETosis was already earlier shown in another study [46]. A pore formation of the neutrophil membrane would result in a positive signal from Live-or-Dye.

However, we cannot exclude the possibility that neutrophils that are alive and NET-activated might be close to dying, as we used fixed endpoints. It cannot be ruled out that such cells, whose membranes are still intact and therefore are categorized as alive, might be in an intermediate stage. Therefore, further studies would be needed, for example, with live imaging. Unfortunately, regarding live-cell imaging, it became evident during the study that, due to the broad emission and excitation ranges of the Live-or-Dye NucFix™, issues can arise when using multiple dyes in one experiment, potentially causing bleed-through into other channels. While this problem can be addressed with configuration adjustments on a confocal microscope, other less complex imaging systems are limited in this regard.

As presented in Fig. 5, the Live-or-Dye NucFix™ can be combined with other dyes in flow cytometry analysis. The findings from the flow cytometry (Fig. 5G) analysis are consistent with the results observed in the NET assays. (Figs. 2–4). In the future, it would be important to test this staining protocol at different time points and with flow cytometry analysis, potentially using an adapted protocol for multispectral imaging flow cytometry [30]. Furthermore, it would be necessary to compare and verify the results using electron microscopy analysis.

We were interested in testing the new staining protocol with samples from a setup that mimics the *in vivo* situation. Therefore, we analyzed the host-pathogen interaction of neutrophils and *S. suis* in a cell culture model of the BCSFB (Fig. 3). In previous studies, we identified that *S. suis* induces NET formation in the CSF compartment of pigs with *S. suis* meningitis, where these NETs entrap *S. suis* [15]. However, without antibiotic treatment, an infected pig will die, suggesting that NET-formation is not an effective defense mechanism during *S. suis* meningitis. This could be attributed to the DNases of *S. suis* and other defense mechanisms against NETs [9,47]. Due to the NET-degrading DNases of *S. suis* [9,47], not only fiber-forming neutrophils were counted, but in all experiments, NET-activated cells were counted (Figs. 1–4).

Interestingly, while *S. suis* induces after two hours NETs in the presence of RPMI, resulting in a high number of alive NET-activated neutrophils (Fig. 2), after four hours the phenotype changes to more impaired NET-activated neutrophils (Fig. 4). Furthermore, neutrophils that have transmigrated into the *S. suis*-infected CSF compartment *in vitro* predominantly undergo NET formation. However, in addition, a high number of NET activated neutrophils die. This phenotype is comparable with the results from four hours of incubation in the presence of the cell culture medium (FCS + Il-8, Fig. 4). Due to the experimental conditions, we were not able to prove whether NET activation comes first, and the neutrophil membrane becomes permeable afterwards, or if these processes occur in parallel. Furthermore, we did not investigate whether the formation of pores by gasdermin E is initiated first, leading to a calcium influx into the neutrophil and PAD4 activation, which results in NETs [44,45]. Therefore, future studies should investigate this in more detail with further improved detection methods like live-cell imaging of the transmigrating

neutrophils. In contrast, after less incubation time (two hours), *S. suis* induced in the presence of the cell culture medium (FCS medium) more alive NET-activated neutrophils (Fig. 2). It is known that FCS influences NET formation, for example, due to the present DNases [48], which could delay the development of a phenotype.

If *S. suis* primarily induces in transmigrated neutrophils NETs and death of the neutrophils, there are no efficiently phagocytically active neutrophils present in the CSF. Few studies investigate the mechanisms by which *S. suis* induces neutrophils to release NETs. It has been shown that certain proteins are overexpressed during *S. suis* stimulation in murine neutrophils, implicating protein kinase C, NADPH oxidase, and myeloperoxidase in the NET induction process, with metalloproteinase-8 acting as an inhibitor. However, no differentiation between vital and suicidal NETs or the number of alive neutrophils was described [49]. Additionally, another study with murine neutrophils demonstrated that TLR2 and TLR4 recognize *S. suis* and trigger NET release through ROS production by NADPH oxidase and activation of p38 MAPK and extracellular signal-regulated kinase pathways. Therefore, it was discussed that *S. suis* induces suicidal NET-formation [50]. However, our data show that *S. suis* induces NET release from both alive and impaired neutrophils and that transmigration into a CSF compartment in an *in vitro* model of the BCSFB shifts the observed phenotype to more impaired NET-activated cells (Fig. 3). This raises the question of why the phenotype changes after transmigration. Possible reasons include I. the increased concentration of *S. suis* in the CSF compartment, leading to a higher amount of the pore-forming cholesterol-dependent cytolysin of *S. suis* (suilysin) [26]; II. cytokines released by the choroid plexus following *S. suis* infection, such as IL-8 or TNF-α [51,52]; III. the influence of the transmigration process on the NET phenotype; and IV. a combination of all three factors.

Our data support the assumption that *S. suis* is the main trigger for increased NET formation *in vitro* and leads to more impaired neutrophils. Obviously, the phenotype of neutrophils is influenced by the length of time the neutrophils are in contact with *S. suis* (Figs. 2 and 4), whereas the influence of the medium is less pronounced. Referring to the possibility that neutrophils may start apoptosis due to a stimulus and then release NETs [44], it is also conceivable that the pores formed by suilysin facilitate a calcium influx into the neutrophils, which then activates PAD4 and leads to the formation of NETs. The significantly increased number of neutrophils that are NET-releasing and impaired was also observed in the 4-h assay without transmigration (Fig. 4). In this assay, the MOI is very low (MOI = 2). Another study demonstrated that at this MOI, the release of lactate dehydrogenase (LDH) during a 4-h incubation is very low, and only an MOI of 20 produces significant LDH release from neutrophils [53]. Future studies could analyze this aspect more deeply by testing mutants and determining additional parameters such as LDH.

Transferred to *in vivo*, factors that keep *S. suis* out of the CSF may be beneficial for the host, as *S. suis* multiplies in CSF, and transmigrated neutrophils in our *in vitro* model are presumably killed over time without an efficient counteracting by NETs. This is supported by the fact that prolonged contact with *S. suis* probably leads to more NET activated and impaired cells (Figs. 2 and 4). From *in vivo* data, we know that neutrophils infiltrating the CSF of *S. suis* infected pigs form NETs [15,19]. However, there is no data available that distinguishes between impaired and alive or vital and suicidal NETosis. Future work could investigate this in more detail and therefore allow a comparison of *in vivo* data and *in vitro* data generated inside the presented cell culture model of the BCSFB. Future studies could investigate NET phenotypes in the CSF compartment *in vivo* as well as in the BCSFB model, potentially using different inhibitors. However, since we did not observe a high number of impaired neutrophils in the CSF compartment after transmigration in the absence of *S. suis* infection (Fig. 3), the transmigration process itself does not appear to be the sole explanation. This aligns well with a study by Mohanty et al., where massive NETs

were visualized in the CSF of *S. pneumoniae*-infected humans using immunofluorescence microscopy and elastase detection [54]. However, in other patients with viral meningitis, neuroborreliosis, or subarachnoid hemorrhage, neutrophils were detected in the CSF, but no NETs were observed [54]. Therefore, it is evident that neutrophils infiltrating the CSF do not universally respond with massive NET release during infections. However, it's important to note that vital NETs were not quantified in the study by Mohanty et al.

This study has strengths and limitations. The staining method we have described initially allows the identification of neutrophils releasing NETs through the classical staining with the DNA/histone-1 complex antibody. In these NET positive cells, the second staining with the dye Live-or-Dye NucFix™ Red staining can then be used to categorize them into "alive" and "impaired" cells. However, we would like to emphasize that we do not equate a lack of staining with Live-or-Dye NucFix™ Red staining with "vital" NETosis [27]. For this term, validation with other methods, particularly electron microscopy analysis, would be necessary. Rather, we view this staining as a new tool to better address mechanistic questions in the future. The new staining protocol is a simpler, faster, and more cost-efficient method compared to conventional electron microscopy, and it allows to quantify impaired and alive neutrophils for a first screening.

Whereas on the one hand, this staining method has the benefit that impaired and alive cells can be visualized in fixed samples, on the other hand, it cannot be ruled out that intermediate stages of NET formation may not yet be positive for Live-or-Dye NucFix™ Red staining. This is also due to the fact that fixed time points were used, and unfortunately, no live imaging was performed. This is mainly due to technical limitations: The dye Live-or-Dye NucFix™ Red staining could be used in live imaging; however, the wide fluorescence range in excitation and emission of the staining leads to several problems in the correct settings for fluorescence imaging in combination with other fluorophores. In addition, the cell culture with filter inserts is only established with specific plastic dishes, and live imaging with filter inserts is challenging. However, future studies could focus on this to specifically investigate when the transmigrated neutrophils turn to death. This could also be combined with fluorescent bacteria to visualize phagocytosed bacteria.

Through the Live-or-Dye NucFix™ Red staining, cells are categorized into "alive" and "impaired" cells based on their membrane integrity. We have paid special attention to the release of NETs by *S. suis*. However, since no inhibitors were used to, for example, inhibit ROS-dependent NET release, specific NETosis mechanisms or pathways cannot be associated with the identified phenotypes. Therefore, the findings should be interpreted as descriptive rather than mechanistic and require further validation using additional specific approaches and techniques such as mass spectrometry, which would be needed to better contextualize the collected data.

Due to the fact that the cell culture under infection conditions does not exceed this 5-h infection period (with four hours of neutrophil transmigration), and the medium in the CSF compartment remains constant (including all changes related to bacterial growth and metabolism), the results must be interpreted with caution in relation to later stages of *S. suis* meningitis *in vivo*. However, one strength of the investigation of the *S. suis* neutrophil interaction in a cell culture model that closely mimics *in vivo* conditions, allows for the generation of new hypotheses. In our cell culture model, we found a positive correlation between the number of bacteria and the number of NET-activated and impaired neutrophils. Based on the literature described above [44,45], it can be hypothesized that these neutrophils have undergone a second cell death. Therefore, they are no longer capable of continuing to fight the infection, leading to increased bacterial growth. Additionally, we observed a negative correlation between the number of bacteria and the number of NET-activated and alive neutrophils. According to the literature, it can be hypothesized that these neutrophils can still perform further antimicrobial activities and are able to combat the infection. However,

this interpretation remains speculative, and future studies need to provide mechanistic validation to test these hypotheses.

In this study, the analysis was performed exclusively in *in vitro* assays using porcine neutrophils. Future studies should analyze *in vivo* data, such as freshly drawn CSF samples from pigs with *S. suis* meningitis. A challenge of the staining protocol, however, is that samples must be transported to a laboratory immediately to begin the Live-or-Dye staining of cytospins as soon as possible, since cells that are still alive at the time of sampling may die shortly thereafter. Fixation of the samples is not possible before the Live-or-Dye staining. Additionally, the staining should be validated in other species, such as humans. While a human BCSFB system is available and has been tested with *S. suis* [15], the porcine system offers the additional advantage of permitting the use of blood and CSF from pigs [19], which is challenging, especially for CSF usage, in the human model. This capability would allow future studies to explore mechanistic questions, for example, by testing *S. suis* mutants known to influence NET release or neutrophil survival [26].

5 Conclusion

To gain insight into the specific immune mechanisms involved in infection, it is crucial to differentiate between vital and suicidal NETosis in neutrophils. By utilizing a novel staining protocol, both alive and impaired cells can be visualized alongside NET formation. This method offers a quick and straightforward pre-screening method before proceeding to more costly and time-intensive electron microscopy analyses. In an *in vitro* model of the BCSFB, we demonstrated that infection with *S. suis* 10 predominantly induces NET-formation with impaired neutrophils. This finding has significant implications for the immune response, as only alive neutrophils are capable of executing additional defense mechanisms such as phagocytosis.

Acknowledgement: We would like to thank Marita Meurer, PhD (Institute of Biochemistry, University of Veterinary Medicine Hannover), for her technical assistance in this project with the cell culture and flow cytometry. We also thank Rabea Imker and Silke Akhdar (both Institute of Biochemistry, University of Veterinary Medicine Hannover) for the technical assistance with the bacteria and neutrophils. *S. suis* 10 was kindly provided by Hilde Smith (Wageningen, GE, the Netherlands). We thank the staff of the Mario Klos slaughterhouse (Nienhagen) for their assistance in collecting the blood samples. Laura Schaltz was supported by the Hannover Graduate School for Neurosciences, Infection Medicine and Veterinary Sciences (HGNI) of the University of Veterinary Medicine Hannover (TiHo).

Funding Statement: This research was funded by the German Research Foundation (DFG), grant number BU 3523/3-1 (Nicole de Buhr received the grant).

Author Contributions: The authors confirm contribution to the paper as follows: Conceptualization, Nicole de Buhr; methodology, Nicole de Buhr, Simon Lassnig, Laura Schaltz; validation, Laura Schaltz, Simon Lassnig, Nicole de Buhr; formal analysis, Laura Schaltz, Nicole de Buhr; investigation, Laura Schaltz, Simon Lassnig, Karola Schlote, Nicole de Buhr; resources, Nicole de Buhr, Christian Schwerk, Horst Schroten; data curation, Laura Schaltz, Nicole de Buhr; writing—original draft preparation, Laura Schaltz, Nicole de Buhr; writing—review and editing, all authors; visualization, Laura Schaltz, Nicole de Buhr; supervision, Nicole de Buhr, Simon Lassnig; project administration, Nicole de Buhr; funding acquisition, Nicole de Buhr. All authors reviewed and approved the final version of the manuscript.

Availability of Data and Materials: The data that support the findings of this study are available from the corresponding author [Nicole de Buhr], upon reasonable request.

Ethics Approval: The study did not include human subjects. The study included blood from pigs. This blood was collected from healthy pigs that were euthanized to collect several biological samples for *in vitro* experiments. This procedure follows the German animal welfare law and was registered at the University of Veterinary Medicine Hannover, Germany with the following numbers: TiHo-T-2024-16 and TiHo-T-2025-2. In addition, blood was collected from pigs at the slaughterhouse from healthy pigs during the slaughter process. All of Laura Schaltz work within the scope of her PhD, involving material from euthanized pigs or the use of biological materials from slaughterhouse

waste, was reported to the animal welfare officer of the University of Veterinary Medicine Hannover, Germany and registered under the number TVT-2025-P-31.

Conflicts of Interest: The authors declare no conflicts of interest.

Abbreviations

BCSFB	Blood-cerebrospinal fluid barrier
CD	Methyl-β-cyclodextrin
CFU/mL	Colony forming units per mL
CSF	Cerebrospinal fluid
DCF	2′,7′-Dichlorodihydrofluorescein diacetate
DMSO	Dimethyl sulfoxide
DNA/histone 1	Mouse monoclonal antibody against DNA/histone 1 complexes
FCS	Fetal calf serum
Live-or-Dye	Live-or-Dye NucFix™ Red Staining Kit
MOI	Multiplicity of infection
NETs	Neutrophil extracellular traps
OD	Optical density
PAD4	Peptidyl arginine deiminase 4
PBS	Phosphate buffered saline
PCP-R	Choroid plexus epithelial cells
PFA	Paraformaldehyde
ROS	Reactive oxygen species
RPMI	Rosewell Park Memorial Institute Medium
S. suis	*Streptococcus suis*
S. suis 10	*Streptococcus suis* strain 10
TEER	Transepithelial electrical resistance
THB	Todd Hewitt Broth medium

Appendix A

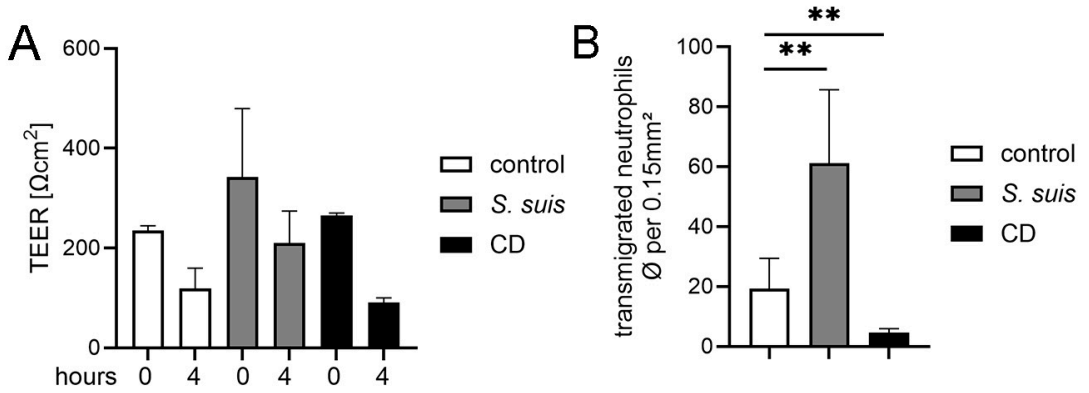

Figure A1: *Cont.*

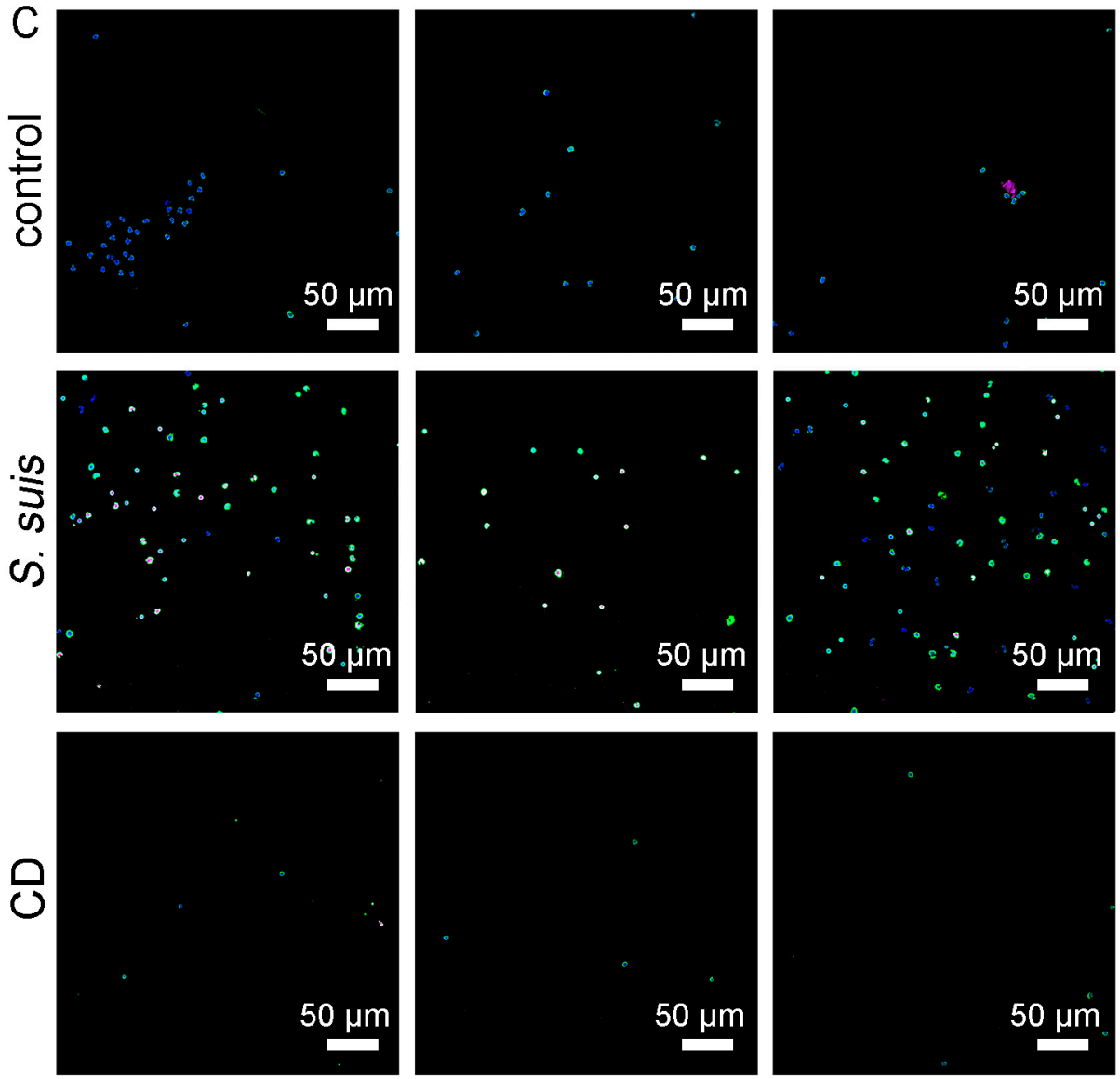

Figure A1: CD does not induce neutrophil transmigration in the BCSFB model and negatively influences the barrier integrity: (**A**–**C**) A control experiment of the BCSFB model was conducted to investigate the influence of CD as a potential positive control for NET release. (**A**) Barrier integrity was determined by measuring the TEER. Data is presented as the mean ± SD, n = 2 independent filters. Statistical analysis: Was not calculated, as only two samples are shown per group. (**B**) Transmigrated neutrophils were counted after staining the NETs on the coverslips inserted in the CSF compartment using confocal fluorescence microscopy images (n = 6 images per sample). Data are presented as the mean ± SD. Statistical analysis: Unpaired Student's *t*-test (**$p < 0.01$). (**C**) Representative images of transmigrated neutrophils after four hours. Blue = DNA (Hoechst 33342), green = NET marker (DNA/Histone1), magenta = impaired cells (Live-or-Dye).

References

1. Segura M, Aragon V, Brockmeier S, Gebhart C, Greeff A, Kerdsin A, et al. Update on *Streptococcus suis* research and prevention in the era of antimicrobial restriction: 4th International workshop on *S. suis*. Pathogens. 2020;9:374. [CrossRef].

2. Brizuela J, Kajeekul R, Roodsant TJ, Riwload A, Boueroy P, Pattanapongpaibool A, et al. *Streptococcus suis* outbreak caused by an emerging zoonotic strain with acquired multi-drug resistance in Thailand. Microb Genom. 2023;9(2):000952. [CrossRef].
3. Williams AE, Blakemore WF. Pathogenesis of meningitis caused by *Streptococcus suis* type 2. J Infect Dis. 1990;162:474–81. [CrossRef].
4. Shechter R, London A, Schwartz M. Orchestrated leukocyte recruitment to immune-privileged sites: Absolute barriers versus educational gates. Nat Rev Immunol. 2013;13:206–18. [CrossRef].
5. Wolburg H, Paulus W. Choroid plexus: Biology and pathology. Acta Neuropathol. 2010;119:75–88. [CrossRef].
6. Prasad R, Kapoor R, Srivastava R, Mishra OP, Singh TB. Cerebrospinal fluid TNF-α, IL-6, and IL-8 in children with bacterial meningitis. Pediatr Neurol. 2014;50:60–5. [CrossRef].
7. Brinkmann V. Neutrophil extracellular traps kill bacteria. Science. 2004;303:1532–5. [CrossRef].
8. Ley K, Hoffman HM, Kubes P, Cassatella MA, Zychlinsky A, Hedrick CC, et al. Neutrophils: New insights and open questions. Sci Immunol. 2018;3(30):eaat4579. [CrossRef].
9. de Buhr N, Neumann A, Jerjomiceva N, von Köckritz-Blickwede M, Baums CG. *Streptococcus suis* DNase SsnA contributes to degradation of neutrophil extracellular traps (NETs) and evasion of NET-mediated antimicrobial activity. Microbiology. 2014;160:385–95. [CrossRef].
10. Fontaine MC, Perez-Casal J, Willson PJ. Investigation of a novel DNase of *Streptococcus suis* serotype 2. Infect Immun. 2004;72:774–81. [CrossRef].
11. Pilsczek FH, Salina D, Poon KKH, Fahey C, Yipp BG, Sibley CD, et al. A novel mechanism of rapid nuclear neutrophil extracellular trap formation in response to staphylococcus aureus. J Immunol. 2010;185:7413–25. [CrossRef].
12. Tan C, Aziz M, Wang P. The vitals of NETs. J Leukoc Biol. 2021;110:797–808. [CrossRef].
13. Yipp BG, Petri B, Salina D, Jenne CN, Scott BNV, Zbytnuik LD, et al. Infection-induced NETosis is a dynamic process involving neutrophil multitasking *in vivo*. Nat Med. 2012;18:1386–93. [CrossRef].
14. Yipp BG, Kubes P. NETosis: How vital is it? Blood. 2013;122:2784–94. [CrossRef].
15. de Buhr N, Reuner F, Neumann A, Stump-Guthier C, Tenenbaum T, Schroten H, et al. Neutrophil extracellular trap formation in the *Streptococcus suis*-infected cerebrospinal fluid compartment. Cell Microbiol. 2017;19:e12649. [CrossRef].
16. Bonilla MC, Quiros ON, Wendt M, Hennig-Pauka I, Mörgelin M, von Köckritz-Blickwede M, et al. New insights into neutrophil extracellular trap (NETs) formation from porcine neutrophils in response to bacterial infections. Int J Mol Sci. 2022;23:8953. [CrossRef].
17. Panpaeng C, Kamolvit W, Karaketklang K, Jitmuang A. Clinical characteristics and trends in the antimicrobial susceptibility profile of *Streptococcus suis* infections in a large tertiary hospital, Thailand, 2007–2023. PLoS Negl Trop Dis. 2025;19:e0013110. [CrossRef].
18. Liedel C, Rieckmann K, Baums CG. A critical review on experimental *Streptococcus suis* infection in pigs with a focus on clinical monitoring and refinement strategies. BMC Vet Res. 2023;19:188. [CrossRef].
19. Meurer M, Öhlmann S, Bonilla MC, Valentin-Weigand P, Beineke A, Hennig-Pauka I, et al. Role of bacterial and host dnases on host-pathogen interaction during *Streptococcus suis* meningitis. Int J Mol Sci. 2020;21:5289. [CrossRef].
20. Schroten M, Hanisch FG, Quednau N, Stump C, Riebe R, Lenk M, et al. A novel porcine *in vitro* model of the blood-cerebrospinal fluid barrier with strong barrier function. PLoS One. 2012;7(6):e39835. [CrossRef].
21. Lauer AN, März M, Meyer S, Meurer M, de Buhr N, Borkowski J, et al. Optimized cultivation of porcine choroid plexus epithelial cells, a blood–cerebrospinal fluid barrier model, for studying granulocyte transmigration. Lab Investig. 2019;99:1245–55. [CrossRef].
22. Breitfelder AK, Schrödl W, Rungelrath V, Baums CG, Alber G, Schütze N, et al. Immunoglobulin M-degrading enzyme of *Streptococcus suis* (IdeSsuis) impairs porcine B cell signaling. Front Immunol. 2023;14:1122808. [CrossRef].
23. Smith HE, Damman M, Van Der Velde J, Wagenaar F, Wisselink HJ, Stockhofe-Zurwieden N, et al. Identification and characterization of the cps locus of *Streptococcus suis* serotype 2: The capsule protects against phagocytosis and is an important virulence factor. Infect Immun. 1999;67:1750–6. [CrossRef].

24. Close B, Banister K, Baumans V, Bernoth EM, Bromage N, Bunyan J, et al. Recommendations for euthanasia of experimental animals: Part 2. DGXT of the European Commission. Lab Anim. 1997;31:1–32. [CrossRef].
25. Srinivasan B, Kolli AR, Esch MB, Abaci HE, Shuler ML, Hickman JJ. TEER measurement techniques for *in vitro* barrier model systems. J Lab Autom. 2015;20:107–26. [CrossRef].
26. Bleuzé M, Gottschalk M, Segura M. Neutrophils in *Streptococcus suis* infection: From host defense to pathology. Microorganisms. 2021;9(11):2392. [CrossRef].
27. Fuchs TA, Abed U, Goosmann C, Hurwitz R, Schulze I, Wahn V, et al. Novel cell death program leads to neutrophil extracellular traps. J Cell Biol. 2007;176:231–41. [CrossRef].
28. Thiam HR, Wong SL, Wagner DD, Waterman CM. Cellular mechanisms of NETosis. Annu Rev Cell Dev Biol. 2020;36:191–218. [CrossRef].
29. Wang H, Kim SJ, Lei Y, Wang S, Wang H, Huang H, et al. Neutrophil extracellular traps in homeostasis and disease. Signal Transduct Target Ther. 2024;9:235. [CrossRef].
30. Zhao W, Fogg DK, Kaplan MJ. A novel image-based quantitative method for the characterization of NETosis. J Immunol Methods. 2015;423:104–10. [CrossRef].
31. Schneck E, Mallek F, Schiederich J, Kramer E, Markmann M, Hecker M, et al. Flow cytometry-based quantification of neutrophil extracellular traps shows an association with hypercoagulation in septic shock and hypocoagulation in postsurgical systemic inflammation—A proof-of-concept study. J Clin Med. 2020;9:174. [CrossRef].
32. Masuda S, Shimizu S, Matsuo J, Nishibata Y, Kusunoki Y, Hattanda F, et al. Measurement of NET formation *in vitro* and *in vivo* by flow cytometry. Cytom Part A. 2017;91:822–9. [CrossRef].
33. Rayes RF, Mouhanna JG, Nicolau I, Bourdeau F, Giannias B, Rousseau S, et al. Primary tumors induce neutrophil extracellular traps with targetable metastasis-promoting effects. JCI Insight. 2019;4(16):e128008. [CrossRef].
34. Pelletier MGH, Szymczak K, Barbeau AM, Prata GN, O'Fallon KS, Gaines P. Characterization of neutrophils and macrophages from *ex vivo*-cultured murine bone marrow for morphologic maturation and functional responses by imaging flow cytometry. Methods. 2017;112:124–46. [CrossRef].
35. Lelliott PM, Momota M, Lee MSJ, Kuroda E, Iijima N, Ishii KJ, et al. Rapid quantification of NETs *in vitro* and in whole blood samples by imaging flow cytometry. Cytom Part A. 2019;95:565–78. [CrossRef].
36. Zharkova O, Tay SH, Lee HY, Shubhita T, Ong WY, Lateef A, et al. A flow cytometry-based assay for high-throughput detection and quantification of neutrophil extracellular traps in mixed cell populations. Cytom Part A. 2019;95:268–78. [CrossRef].
37. Mehrpouya-Bahrami P, Moriarty AK, De Melo P, Keeter WC, Alakhras NS, Nelson AS, et al. STAT4 is expressed in neutrophils and promotes antimicrobial immunity. JCI Insight. 2021;6(14):e141326. [CrossRef].
38. Rungelrath V, Öhlmann S, Alber G, Schrödl W, von Köckritz-Blickwede M, de Buhr N, et al. Survival of *Streptococcus suis* in porcine blood is limited by the antibody- and complement-dependent oxidative burst response of granulocytes. Infect Immun. 2020;88:1–21. [CrossRef].
39. Bleuzé M, Lavoie J-P, Bédard C, Gottschalk M, Segura M. Encapsulated *Streptococcus suis* impairs optimal neutrophil functions which are not rescued by priming with colony-stimulating factors. PLoS One. 2024;19:e0296844. [CrossRef].
40. Xie H, Li Y, Fang Q, Xie H, Huang J, Wu Z, et al. SodA promotes immune evasion of *Streptococcus suis* by suppressing ROS accumulation and GSDMD-mediated mitochondrial disruption in neutrophils. Microbiol Spectr. 2026;14:e0190125. [CrossRef].
41. Liu ML, Lyu X, Werth VP. Recent progress in the mechanistic understanding of NET formation in neutrophils. FEBS J. 2022;289(14):3954–66. [CrossRef].
42. Thiam HR, Wong SL, Qiu R, Kittisopikul M, Vahabikashi A, Goldman AE, et al. NETosis proceeds by cytoskeleton and endomembrane disassembly and PAD4-mediated chromatin decondensation and nuclear envelope rupture. Proc Natl Acad Sci U S A. 2020;117:7326–37. [CrossRef].
43. Hsu AY, Huang Q, Liu F, Balasubramanian A, Luo HR. Neutrophil death-more than meets the eye. Exp Hematol. 2025;150:104857. [CrossRef].
44. Zhu YP, Speir M, Tan Z, Lee JC, Nowell CJ, Chen AA, et al. NET formation is a default epigenetic program controlled by PAD4 in apoptotic neutrophils. Sci Adv. 2023;9:eadj1397. [CrossRef].
45. Souza FW, Miao EA. Neutrophils only die twice. Sci Adv. 2023;9(51):eadm8715. [CrossRef].

46. Sollberger G, Choidas A, Burn GL, Habenberger P, Di Lucrezia R, Kordes S, et al. Gasdermin D plays a vital role in the generation of neutrophil extracellular traps. Sci Immunol. 2018;3(26):eaar6689. [CrossRef].
47. de Buhr N, Stehr M, Neumann A, Naim HY, Valentin-Weigand P, von Köckritz-Blickwede M, et al. Identification of a novel DNase of *Streptococcus suis* (EndAsuis) important for neutrophil extracellular trap degradation during exponential growth. Microbiology. 2015;161:838–50. [CrossRef].
48. von Köckritz-Blickwede M, Chow OA, Nizet V. Fetal calf serum contains heat-stable nucleases that degrade neutrophil extracellular traps. Blood. 2009;114:5245–6. [CrossRef].
49. Wang X, Zhao J, Cai C, Tang X, Fu L, Zhang A, et al. A label-free quantitative proteomic analysis of mouse neutrophil extracellular trap formation induced by *Streptococcus suis* or phorbol myristate acetate (PMA). Front Immunol. 2018;9:1–14. [CrossRef].
50. Ma F, Chang X, Wang G, Zhou H, Ma Z, Lin H, et al. *Streptococcus suis* serotype 2 stimulates neutrophil extracellular traps formation via activation of p38 MAPK and ERK1/2. Front Immunol. 2018;9:2854. [CrossRef].
51. Schwerk C, Adam R, Borkowski J, Schneider H, Klenk M, Zink S, et al. *In vitro* transcriptome analysis of porcine choroid plexus epithelial cells in response to *Streptococcus suis*: Release of pro-inflammatory cytokines and chemokines. Microbes Infect. 2011;13:953–62. [CrossRef].
52. Papayannopoulos V, Metzler KD, Hakkim A, Zychlinsky A. Neutrophil elastase and myeloperoxidase regulate the formation of neutrophil extracellular traps. J Cell Biol. 2010;191:677–91. [CrossRef].
53. Chabot-Roy G, Willson P, Segura M, Lacouture S, Gottschalk M. Phagocytosis and killing of *Streptococcus suis* by porcine neutrophils. Microb Pathog. 2006;41:21–32. [CrossRef].
54. Mohanty T, Fisher J, Bakochi A, Neumann A, Cardoso JFP, Karlsson CAQ, et al. Neutrophil extracellular traps in the central nervous system hinder bacterial clearance during pneumococcal meningitis. Nat Commun. 2019;10:1667. [CrossRef].